

4. Drilon A, Wang L, Hasanovic A, Suehara Y, Lipson D, Stephens P, et al. Response to Cabozantinib in Patients with RET Fusion-Positive Lung Adenocarcinomas. *Cancer Discov* 2013;3:630-5.
5. Takeuchi K, Soda M, Togashi Y, Suzuki R, Sakata S, Hatano S, et al. RET, ROS1 and ALK fusions in lung cancer. *Nat Med* 2012;18:378-81.
6. Mano H. ALKoma: a cancer subtype with a shared target. *Cancer Discov* 2012;2:495-502.
7. Lipson D, Capelletti M, Yelensky R, Otto G, Parker A, Jarosz M, et al. Identification of new ALK and RET gene fusions from colorectal and lung cancer biopsies. *Nat Med* 2012;18:382-4.
8. Kohno T, Ichikawa H, Totoki Y, Yasuda K, Hiramoto M, Nammo T, et al. KIF5B-RET fusions in lung adenocarcinoma. *Nat Med* 2012;18:375-7.
9. Ju YS, Lee WC, Shin JY, Lee S, Bleazard T, Won JK, et al. A transforming KIF5B and RET gene fusion in lung adenocarcinoma revealed from whole-genome and transcriptome sequencing. *Genome Res* 2012;22:436-45.
10. Oxnard GR, Binder A, Janne PA. New targetable oncogenes in non-small-cell lung cancer. *J Clin Oncol* 2013;31:1097-104.
11. Kohno T, Tsuta K, Tsuchihara K, Nakaoku T, Yoh K, Goto K. RET fusion gene: Translation to personalized lung cancer therapy. *Cancer Sci* 2013;104:1396-400.
12. Travis WD, Brambilla E, Riely GJ. New pathologic classification of lung cancer: relevance for clinical practice and clinical trials. *J Clin Oncol* 2013;31:992-1001.
13. Travis WD, Brambilla E, Noguchi M, Nicholson AG, Geisinger KR, Yatabe Y, et al. International association for the study of lung cancer/american thoracic society/european respiratory society international multidisciplinary classification of lung adenocarcinoma. *J Thorac Oncol* 2011;6:244-85.
14. Tsuta K, Kawago M, Inoue E, Yoshida A, Takahashi F, Sakurai H, et al. The utility of the proposed IASLC/ATS/ERS lung adenocarcinoma subtypes for disease prognosis and correlation of driver gene alterations. *Lung Cancer* 2013;81:371-6.
15. Warth A, Muley T, Meister M, Stenzinger A, Thomas M, Schirmer P, et al. The novel histologic International Association for the Study of Lung Cancer/American Thoracic Society/European Respiratory Society classification system of lung adenocarcinoma is a stage-independent predictor of survival. *J Clin Oncol* 2012;30:1438-46.
16. Yoshizawa A, Motoi N, Riely GJ, Sima CS, Gerald WL, Kris MG, et al. Impact of proposed IASLC/ATS/ERS classification of lung adenocarcinoma: prognostic subgroups and implications for further revision of staging based on analysis of 514 stage I cases. *Mod Pathol* 2011;24:653-64.
17. Travis WD, Brambilla E, Muller-Hermelink HK, Harris CC, editors. World Health Organization classification of tumors: Pathology and genetics, tumours of lung, pleura, thymus and heart. Lyon, France: IARC Press; 2004.
18. Kim D, Salzberg SL. TopHat-Fusion: an algorithm for discovery of novel fusion transcripts. *Genome Biol* 2011;12:R72.
19. Falls DL. Neuregulins: functions, forms, and signaling strategies. *Exp Cell Res* 2003;284:14-30.
20. Fleck D, van Bebber F, Colombo A, Galante C, Schwenk BM, Rabe L, et al. Dual cleavage of neuregulin 1 type III by BACE1 and ADAM17 liberates its EGF-like domain and allows paracrine signaling. *J Neurosci* 2013;33:7856-69.
21. Dislich B, Lichtenthaler SF. The membrane-bound aspartyl protease BACE1: molecular and functional properties in Alzheimer's disease and beyond. *Front Physiol* 2012;3:8.
22. Majem M, Pallares C. An update on molecularly targeted therapies in second- and third-line treatment in non-small cell lung cancer: focus on EGFR inhibitors and anti-angiogenic agents. *Clin Transl Oncol* 2013;15:343-57.
23. Perez EA, Spano JP. Current and emerging targeted therapies for metastatic breast cancer. *Cancer* 2012;118:3014-25.
24. Nelson V, Ziehr J, Agulnik M, Johnson M. Afatinib: emerging next-generation tyrosine kinase inhibitor for NSCLC. *Onco Targets Ther* 2013;6:135-43.
25. Palanisamy N, Ateeq B, Kalyana-Sundaram S, Pflueger D, Ramnarayanan K, Shankar S, et al. Rearrangements of the RAF kinase pathway in prostate cancer, gastric cancer and melanoma. *Nat Med* 2010;16:793-8.
26. Wilhelm SM, Adnane L, Newell P, Villanueva A, Llovet JM, Lynch M. Preclinical overview of sorafenib, a multikinase inhibitor that targets both Raf and VEGF and PDGF receptor tyrosine kinase signaling. *Mol Cancer Ther* 2008;7:3129-40.
27. Kettle R, Simmons J, Schindler F, Jones P, Dicker T, Dubois G, et al. Regulation of neuregulin 1beta1-induced MUC5AC and MUC5B expression in human airway epithelium. *Am J Respir Cell Mol Biol* 2010;42:472-81.

Clinical Cancer Research

Druggable Oncogene Fusions in Invasive Mucinous Lung Adenocarcinoma

Takashi Nakaoku, Koji Tsuta, Hitoshi Ichikawa, et al.

Clin Cancer Res 2014;20:3087-3093. Published OnlineFirst April 11, 2014.

Updated version	Access the most recent version of this article at: doi: 10.1158/1078-0432.CCR-14-0107
Supplementary Material	Access the most recent supplemental material at: http://clincancerres.aacrjournals.org/content/suppl/2014/04/16/1078-0432.CCR-14-0107.DC1.html

Cited Articles	This article cites by 26 articles, 9 of which you can access for free at: http://clincancerres.aacrjournals.org/content/20/12/3087.full.html#ref-list-1
-----------------------	--

E-mail alerts	Sign up to receive free email-alerts related to this article or journal.
Reprints and Subscriptions	To order reprints of this article or to subscribe to the journal, contact the AACR Publications Department at pubs@aacr.org .
Permissions	To request permission to re-use all or part of this article, contact the AACR Publications Department at permissions@aacr.org .

A mouse model of *KIF5B-RET* fusion-dependent lung tumorigenesis

Motonobu Saito^{1,2}, Teruhide Ishigame^{1,2}, Koji Tsuta³,
Kensuke Kumamoto², Toshio Imai⁴ and Takashi Kohno^{*1}

¹Division of Genome Biology, National Cancer Center Research Institute, Tokyo 104-0045, Japan, ²Department of Organ Regulatory Surgery, Fukushima Medical University School of Medicine, Fukushima 960-1295, Japan, ³Division of Pathology and Clinical Laboratories, National Cancer Center Hospital, Tokyo, Japan and ⁴Central Animal Division, National Cancer Center Research Institute, Tokyo 104-0045, Japan

*To whom correspondence should be addressed. Tel: +81 3 3542 2511;
Fax: +81 3 3542 0807;
Email: tkkohno@ncc.go.jp

Oncogenic fusion of the *RET* (rearranged during transfection) gene was recently identified as a novel driver gene aberration not only for the development of thyroid carcinoma but also of lung adenocarcinoma, the most frequent histological type of lung cancer. This study constructed and analyzed transgenic mice expressing *KIF5B-RET*, the predominant form of *RET* fusion gene specific for lung adenocarcinoma, under the control of the *SPC* (surfactant protein C) gene promoter. The mice expressed the *KIF5B-RET* fusion gene specifically in lung alveolar epithelial cells, and developed multiple tumors in the lungs. Treatment of the transgenic mice with vandetanib, which is a *RET* tyrosine kinase inhibitor approved by the U.S. Food and Drug Administration for the treatment of thyroid carcinoma, for 8 or 20 weeks led to a marked reduction in the number of lung tumors (3.3 versus 0 and 6.5 versus 0.2 per tissue section, respectively; $P < 0.01$, *t*-test). The results suggest that the *RET* fusion functions as a driver for the development of lung tumors, whose growth is inhibited by *RET* tyrosine kinase inhibitors.

Introduction

Lung adenocarcinoma (LADC) is the most common histological type of lung cancer and its incidence is increasing in both Asian and Western countries (1). Recent genome-wide sequencing analyses identified somatic genomic aberrations associated with LADC. Activating mutations in several protein kinase genes, including *EGFR*, *BRAF*, *HER2/ERBB2*, *PIK3CA* and *MET*, function as drivers for LADC development and are potential therapeutic targets (2). Oncogenic fusions of protein tyrosine kinase genes, such as *ALK* and *ROS1*, are also drivers of carcinogenesis (3,4); indeed, their ability to drive tumorigenesis *in vivo* has been shown by constructing and analyzing transgenic mice expressing the *EML4-ALK* and *EZR-ROS1* genes (predominant forms of *ALK* and *ROS1* fusions, respectively) specifically in lung alveolar epithelial cells (5–7).

We and others recently identified oncogenic fusions of the *RET* (rearranged during transfection) gene as a novel driver for the development not only of papillary thyroid carcinoma but also of LADC (8–11). *KIF5B-RET* is the predominant form of *RET* fusion in LADC. Other fusions, including *CCDC6-RET*, *NCOA4-RET* and *TRIM33-RET*, which are detected in papillary thyroid carcinoma, are also found in LADC, although they are minor forms (8,12,13). Previous studies used a conventional NIH3T3 cell assay to demonstrate the transforming activity of the *KIF5B-RET* fusion gene (11,14); however, the ability of *KIF5B-RET* fusion gene to drive tumorigenesis *in vivo* has not been proved.

Abbreviations: CT, computed tomography; HPF, high power field; LADC, lung adenocarcinoma; LPF low power field; SPC, surfactant protein C.

Here, we constructed a transgenic mouse model to examine the oncogenic potential of the *KIF5B-RET* fusion in lung alveolar epithelial cells *in vivo*. The *KIF5B-RET* transgene was expressed in lung epithelial cells under the control of the *SPC* (surfactant protein C) promoter; *SPC* is a gene that is specifically expressed in lung alveolar epithelial cells (5,7). Analysis of this mouse model revealed that the *RET* fusion generates lung tumors *in vivo*, and that tumor formation is suppressed by vandetanib, a *RET* tyrosine kinase inhibitor approved by the U.S. Food and Drug Administration (FDA).

Materials and methods

Generation of transgenic mice

KIF5B-RET (K15; R12) cDNA bearing a FLAG-tag at the N-terminus was ligated into a plasmid vector carrying the *SPC* promoter along with splicing and polyadenylation signals (kindly provided by Dr K Hagiwara of Saitama Medical University (7)). The *RET* cDNA in this plasmid was derived from the longer splicing isoform, *RET51*(15). The expression cassette was then injected into pronuclear-stage embryos from C57BL/6J mice (Unitech Japan). The copy numbers of the transgene were measured by Southern blot analysis of DNA isolated from the tails of the founder mice. Total RNA was isolated from several organs of *KIF5B-RET* transgenic mice (line #1, 25 weeks-of-age) using the RNeasy Mini Kit (Qiagen) and subjected to reverse transcription with SuperScript III reverse transcriptase (Invitrogen) and oligo(dt) primer. The PCR primers used to confirm *KIF5B-RET* cDNA expression were as follows: forward, 5'-ATTAGGTGGGAAGCTGAGAACC-3', and reverse, 5'-CAGGCCCATACAATTTGAT-3'. The primers used for *GAPDH* expression were as follows: forward, 5'-AACTTTGGCATTGTGGAAGG-3', and reverse, 5'-CCC TGT TGCTGTAGCCGTAT-3'. Whole cell lysates were prepared from several organs of #1 line mouse (25 weeks-of-age). The *KIF5B-RET* protein was detected by Western blotting with anti-*RET* (ab134100, Abcam) and anti- β -actin (13E5, #4970, Cell Signaling Technology) antibodies (16).

Mice were maintained in a standard air-conditioned and specific pathogen-free animal room. F2 mice were generated by *in vitro* fertilization using an F1 mouse according to a standard method and then subjected to examination. All animal experiments were approved by the Committee for Ethics of Animal Experimentation of the National Cancer Center, Tokyo, Japan.

Gross anatomical and histopathological examination

Examination of lung tumors in living animals was performed by micro-CT (R-mCT2, Rigaku). All mice were anesthetized with isoflurane prior to and throughout the scans. Gross examination of organ morphology was performed after scheduled killing. Moribund mice showing weight loss or difficulty in moving or breathing were also immediately killed and similarly necropsied. Whole lung tissues were fixed in 10% formalin, embedded in paraffin, sectioned and then stained with hematoxylin and eosin (H&E). Pulmonary proliferative lesions were categorized as hyperplasias, adenomas and adenocarcinomas according to previously established criteria (17).

Immunohistochemical staining (IHC)

Serial paraffin sections of lung tissue were immunostained using an EnVision System-HRP (DAB) (Dako) as previously described (16,18). Primary antibodies against *RET* (1:250, clone 3454_1; Epitomics, Burlingame) and Ki-67 (1:2000, ab15580, Abcam) were used for IHC.

Treatment with a *RET* inhibitor

KIF5B-RET transgenic mice were administered vandetanib (50 mg/kg body weight, gavage, once daily; V-9401, LC Laboratories, MA) or vehicle alone. Treatment started at 39 weeks-of-age (when the *KIF5B-RET* transgenic mice began to develop lung tumors). At 8 (47 weeks-of-age) or 20 (59 weeks-of-age) weeks of treatment, the *KIF5B-RET* transgenic mice were killed and necropsied ($n = 6$ per group; treated and non-treated). One transgenic mouse of vandetanib treatment group accidentally died at week 8.

Statistical analysis

Differences between groups were assessed using an unpaired *t*-test, the Mann-Whitney U-test or Fisher's exact test. All analyses were performed with Prism software (GraphPad Software, San Diego, CA). *P* values <0.05 were considered significant. All data are expressed as the mean \pm SD.

Results

Generation of *KIF5B-RET* transgenic mice

To investigate the role of *KIF5B-RET* in lung tumorigenesis, we generated transgenic mice that specifically expressed the fusion gene in the lung. The transgene construct comprised *KIF5B-RET* (K15; R12) cDNA, the most frequently occurring *RET* fusion variant (13,19), the SPC promoter, an RNA splicing cassette, and a polyadenylation signal (Figure 1A). We obtained nine independent F1 mouse lines, each carrying 5–7 copies of the transgene (Figure 1B, Supplementary Table S1, available at *Carcinogenesis* Online). To investigate lung-specific expression of the transgene, we performed RT-PCR and immunoblot analysis to detect *KIF5B-RET* mRNA and protein, respectively, in transgenic mice from the #1 line carrying approximately six copies of the transgene. *KIF5B-RET* mRNA and protein

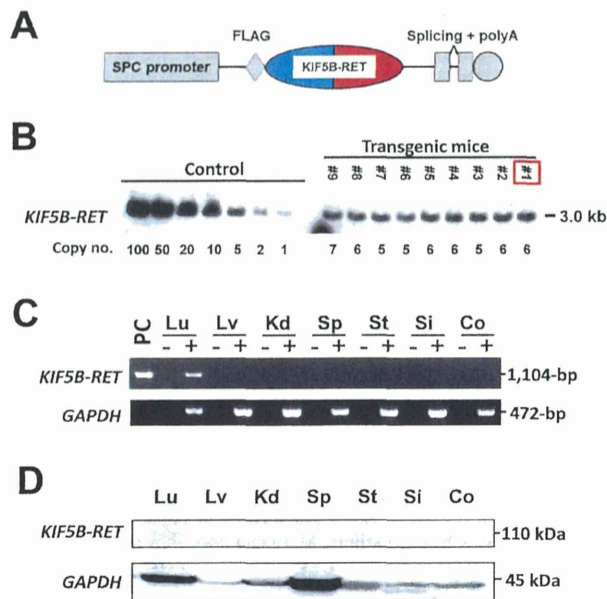


Fig. 1. Lung tumorigenesis in *KIF5B-RET* transgenic mice. (A) Schematic representation of the transgene. A cDNA encoding FLAG-tagged *KIF5B-RET* was inserted between the SPC promoter and the splicing and polyadenylation (polyA) signal sequences. (B) Copy number analysis. Genomic DNA was obtained from the tails of transgenic mice (lines #1–9) generated from pronuclear-stage C57BL/6J embryos and analyzed by Southern blot analysis using a full-length *KIF5B-RET* cDNA probe. Controls comprised mouse genomic DNA with 1, 2, 5, 10, 20, 50 and 100 copies of the transgene per diploid genome. A line #1 mouse (marked in red) was selected to build the transgenic line. (C) *KIF5B-RET* mRNA expression. Oligo(dt)-primed cDNA was synthesized from total RNA isolated from lung (Lu), liver (Lv), kidney (Kd), spleen (Sp), stomach (St), small intestine (Si) and colon (Co) from a mouse from the #1 line (25 weeks-of-age) and subjected to RT-PCR in the presence (+) or absence (–) of reverse transcriptase. RT-PCR was also performed using a human LADC specimen harboring *KIF5B-RET* (positive control, PC). *GAPDH* was used as the control. (D) *KIF5B-RET* protein expression. Whole cell lysates were prepared from lung (Lu), liver (Lv), kidney (Kd), spleen (Sp), stomach (St), small intestine (Si) and colon (Co) from #1 line mouse (25 weeks-of-age) and subjected to western blot analysis with an anti-RET antibody (ab134100, Abcam) that recognizes the C-terminus of the RET polypeptide. β -actin was used as a control.

were specifically detected in the lungs, but not in several other organs (Figure 1C and D).

Development of lung neoplasms in *KIF5B-RET* transgenic mice

The postnatal growth of *KIF5B-RET* transgenic mice was indistinguishable from that of their littermate controls and they did not show any gross abnormalities. To investigate the oncogenic role of the *RET* fusion, we performed scheduled necropsy and histopathological examination of the lungs from 33 F2 mice harboring the transgene and 26 without the transgene. *KIF5B-RET* transgenic mice developed visible nodules on the surface of the lungs. Subsequent histological analysis revealed that the multifocal proliferative pulmonary lesions included hyperplasias, adenomas and adenocarcinomas. *KIF5B-RET* transgenic mice had a significantly higher incidence of lung tumors (adenomas and/or carcinomas) than control mice ($P = 0.002$; log-rank test) (Figure 2A). Computed tomography (CT) revealed progressive enlargement of multiple lung tumors in *KIF5B-RET* transgenic mice with aging, consistent with grossly visible nodules on the surface of the lungs (Figure 2B). At 83 weeks-of-age, all seven transgenic mice examined harbored adenomas and one mouse examined harbored adenocarcinomas. Immunohistochemical analysis using an anti-RET antibody revealed diffuse cytoplasmic granular staining in the adenoma and adenocarcinoma cells (Figure 2C and D). These pulmonary lesions were positive for Ki-67, suggesting that *KIF5B-RET* fusion protein expression is associated with cell proliferative activities. The histopathological features of these lung tumors (e.g. a papillary growth pattern) are similar to those observed in human LADCs harboring the *KIF5B-RET* fusion (20) (Supplementary Table S1, available at *Carcinogenesis* Online).

An FDA-approved *RET* tyrosine kinase inhibitor suppresses the oncogenic activity of the *KIF5B-RET* fusion

We next examined whether a drug that inhibits *RET* tyrosine kinase suppressed lung tumorigenesis in *KIF5B-RET* transgenic mice. As shown in Figure 3A, *KIF5B-RET* transgenic mice were treated with vandetanib (50 mg/kg body weight per day) or with vehicle alone for 8 or 20 weeks. The mice in each group were subsequently necropsied and histopathologically evaluated for pulmonary proliferative lesions by examining a single cross section of lung from each mouse. The majority (83%) of vehicle-treated mice harbored multiple hyperplasias and adenomas compared with 20% of vandetanib-treated mice (Table I). No adenocarcinomas were observed in both of the groups. The number of adenomas per cross section of lung in the vehicle-treated mice at 8 weeks was smaller than that at 20 weeks (3.3 ± 2.5 versus 6.5 ± 3.9), indicating increased occurrence with aging (Figure 3A and B). However, no adenomas were observed in vandetanib-treated mice at 8 weeks and only 0.2 ± 0.4 were observed at 20 weeks (Figure 3B and C), indicating that vandetanib effectively suppresses *RET* fusion-driven lung tumorigenesis.

Discussion

Here, we showed that the *KIF5B-RET* fusion gene is oncogenic in lung alveolar epithelial cells *in vivo*. Pulmonary proliferative lesions, including hyperplasias, adenomas and adenocarcinomas, developed in mice harboring a *RET* fusion transgene. The tumorigenesis was markedly suppressed by vandetanib, an FDA-approved *RET* kinase inhibitor. Thus, this line of transgenic mice is a suitable model for *RET* fusion-driven lung carcinogenesis.

We found that lung tumors developed more slowly in *KIF5B-RET* transgenic mice than in *EMLA-RET* and *EZR-ROS1* transgenic mice, which harbor the same SPC-driven expression system and a similar copy number of transgenes (three and four copies, respectively (5,7)). The reason for this difference in tumor growth is unknown. It may be that the transgenic mice used in this study might express lower levels of the transgene than *EMLA-RET* and

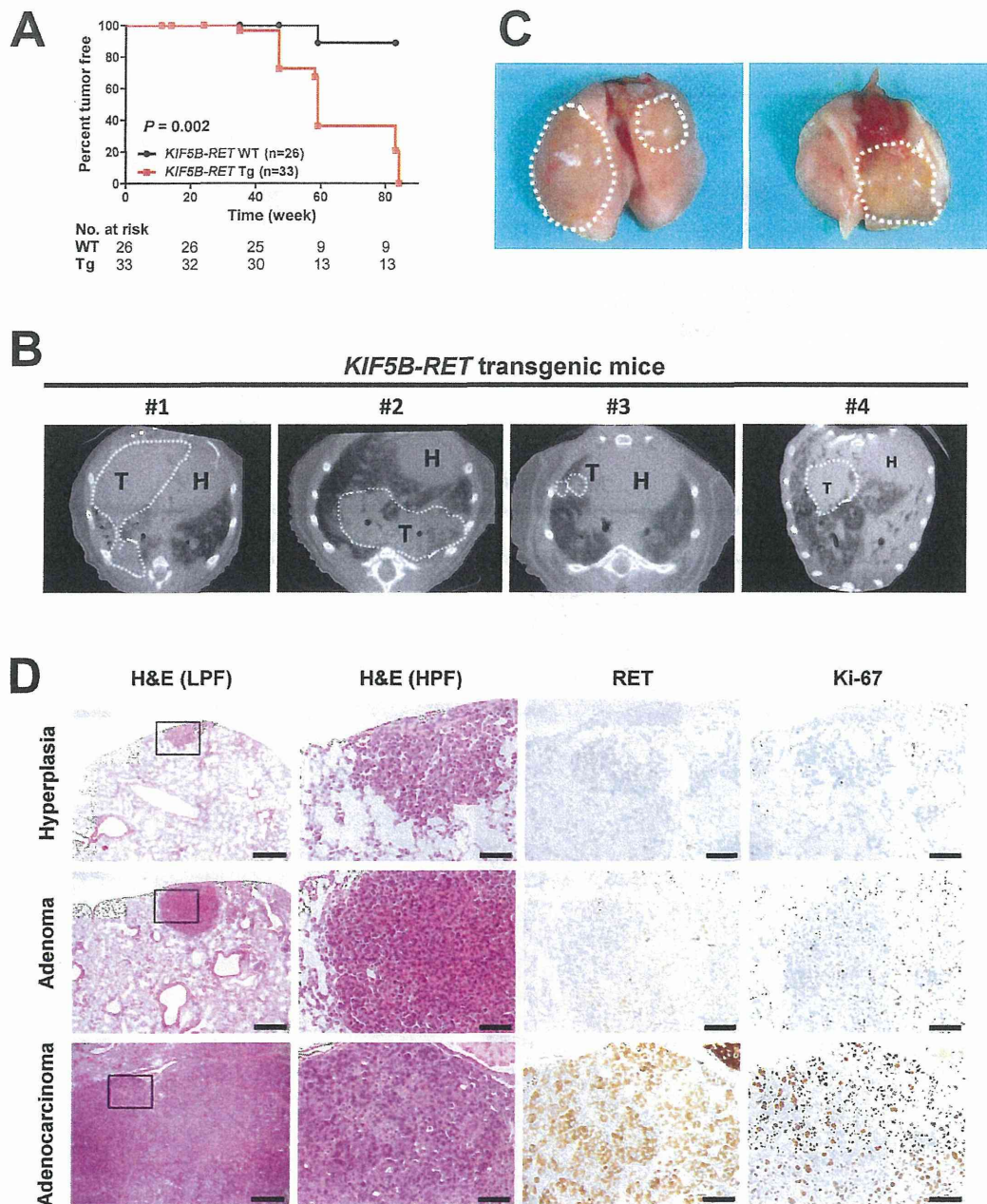


Fig. 2. Development of pulmonary lesions in *KIF5B-RET* transgenic mice. (A) Kaplan–Meier tumor-free survival curves for F2 mice with and without the *KIF5B-RET* transgene. *P* values were calculated using the log-rank test. The number of mice other than those with detectable tumors at the time of necropsy is shown below the curves. (B) Computed tomography images of the lungs from four 75-week-old *KIF5B-RET* transgenic F2 mice. The tumor (T) and the heart (H) are indicated. (C) Representative gross findings in lungs isolated from 83-week-old *KIF5B-RET* transgenic F2 mice. (D) Representative histopathological images of lung hyperplasia, adenoma, and adenocarcinoma in the mice shown in (C). Low and high resolution images of hematoxylin and eosin (H&E)-stained and RET- and Ki-67-immunostained tissues are shown. Scale bar = 500 μ m [H&E low power field (LPF)] and 100 μ m [H&E high power field (HPF); RET and Ki-67].

EZR-ROS1 transgenic mice. Alternatively, the *KIF5B-RET* fusion may be a weaker driver for tumor proliferation than the *EML4-RET* and *EZR-ROS1* fusions. In fact, the latter idea is supported by the results of a recent large-scale screening study that examined *RET* fusion-positive LADCs. The results showed that tumors harboring *RET* fusions were significantly smaller than those harboring *ALK* and *ROS1* fusions (21). Differences in the ability to drive

tumorigenesis might correlate with the time at which visible tumors appear in the lungs.

The utility of several *RET* tyrosine kinase inhibitors such as vandetanib, cabozantinib and E7080 as treatments for *RET* fusion-positive LADC is being examined in clinical trials (8,12), and promising results have been reported in a few patients (13,22). Thus, the therapeutic *in vivo* experiments described herein will complement these clinical trials.

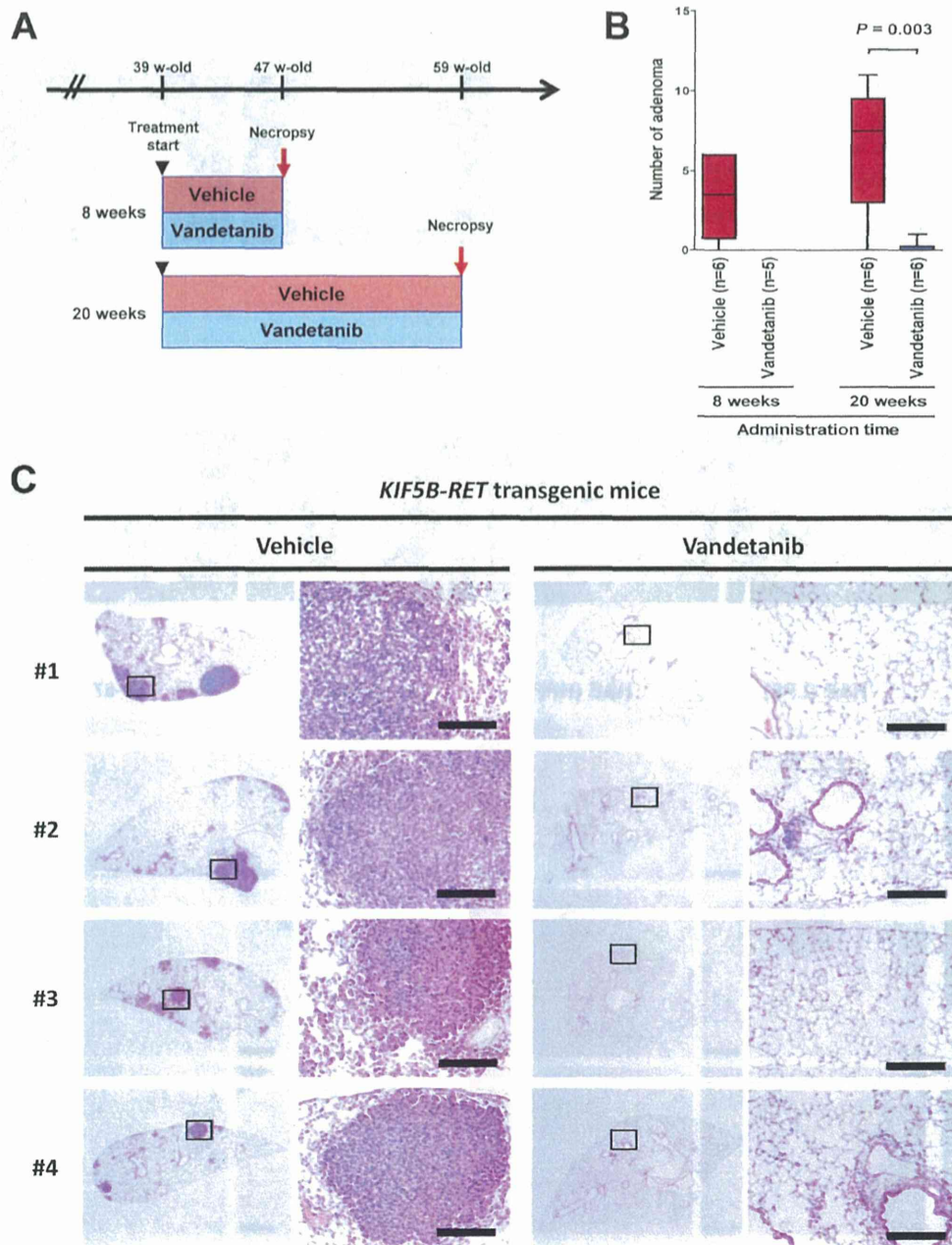


Fig. 3. Administration of vandetanib to *KIF5B-RET* transgenic mice. (A) Treatment schedule for the vandetanib-treated and vehicle (control) groups. The time of necropsy is also shown. One group was necropsied after 8 weeks of treatment (or not) and the other after 20 weeks. (B) Average number of adenomas in the treatment and control groups. Adenomas were counted by examining a single cross section of H&E-stained lung tissue. *P* values were calculated using an unpaired *t*-test. (C) Representative histopathological images showing lung tissue from the 20 week treatment group. Scale bar = 100 μ m. Adenomas are observed only in lungs from control (vehicle-treated) mice.

Table I. Development of lung proliferative lesions in *KIF5B-RET* transgenic mice

Group (according to administration time)	No. of mice examined	No. of mice with hyperplasia	No. of mice with adenoma
8 weeks			
Vehicle	6	5 (83%)	5 (83%)
Vandetanib	5	1 (20%)	0 (0%)
20 weeks			
Vehicle	6	5 (83%)	5 (83%)
Vandetanib	6	0 (0%)	0 (0%)

Supplementary material

Supplementary Table S1 can be found at <http://carcin.oxfordjournals.org/>

Funding

This work was supported in part by Grants-in-Aid from the Ministry of Health, Labor and Welfare for Research for Promotion of Cancer Control Programs(H26-Kakushingan-Ippan-007) and a Grant-in-Aid from the Japan Society for the Promotion of Science (JSPS) for Scientific Research (B) (26293200).

Acknowledgements

We thank Mr N Uchiya and the Animal Core Facility of the National Cancer Center Research Institute for maintaining the mouse colony and technical support for the histological evaluations.

Conflict of Interest Statement: None declared.

References

1. Travis,W.D. *et al.* (2004) *World Health Organization Classification of Tumors; Pathology and Genetics, Tumours of Lung, Pleura, Thymus and Heart*. IARC Press, Lyon.
2. Oxnard,G.R. *et al.* (2013) New targetable oncogenes in non-small-cell lung cancer. *J. Clin. Oncol.*, **31**, 1097–1104.
3. Shaw,A.T. *et al.* (2013) Tyrosine kinase gene rearrangements in epithelial malignancies. *Nat. Rev. Cancer*, **13**, 772–787.
4. Shaw,A.T. *et al.* (2013) ALK in lung cancer: past, present, and future. *J. Clin. Oncol.*, **31**, 1105–1111.
5. Arai,Y. *et al.* (2013) Mouse model for ROS1-rearranged lung cancer. *PLoS One*, **8**, e56010.
6. Chen,Z. *et al.* (2010) Inhibition of ALK, PI3K/MEK, and HSP90 in murine lung adenocarcinoma induced by EML4-ALK fusion oncogene. *Cancer Res.*, **70**, 9827–9836.
7. Soda,M. *et al.* (2008) A mouse model for EML4-ALK-positive lung cancer. *Proc. Natl Acad. Sci. U. S. A.*, **105**, 19893–19897.
8. Mulligan,L.M. (2014) RET revisited: expanding the oncogenic portfolio. *Nat. Rev. Cancer*, **14**, 173–186.
9. Liu,P. *et al.* (2012) Identification of somatic mutations in non-small cell lung carcinomas using whole-exome sequencing. *Carcinogenesis*, **33**, 1270–1276.
10. Lipson,D. *et al.* (2012) Identification of new ALK and RET gene fusions from colorectal and lung cancer biopsies. *Nat. Med.*, **18**, 382–384.
11. Kohno,T. *et al.* (2012) KIF5B-RET fusions in lung adenocarcinoma. *Nat. Med.*, **18**, 375–377.
12. Kohno,T. *et al.* (2013) RET fusion gene: translation to personalized lung cancer therapy. *Cancer Sci.*, **104**, 1396–1400.
13. Dilon,A. *et al.* (2013) Response to Cabozantinib in patients with RET fusion-positive lung adenocarcinomas. *Cancer Discov.*, **3**, 630–635.
14. Takeuchi,K. *et al.* (2012) RET, ROS1 and ALK fusions in lung cancer. *Nat. Med.*, **18**, 378–381.
15. Pasini,A. *et al.* (1997) Oncogenic activation of RET by two distinct FMTC mutations affecting the tyrosine kinase domain. *Oncogene*, **15**, 393–402.
16. Saito,M. *et al.* (2010) Targeted disruption of *Ing2* results in defective spermatogenesis and development of soft-tissue sarcomas. *PLoS One*, **5**, e15541.
17. Nikitin,A.Y. *et al.* (2004) Classification of proliferative pulmonary lesions of the mouse: recommendations of the mouse models of human cancers consortium. *Cancer Res.*, **64**, 2307–2316.
18. Okayama,H. *et al.* (2013) NOS2 enhances KRAS-induced lung carcinogenesis, inflammation and microRNA-21 expression. *Int. J. Cancer*, **132**, 9–18.
19. Mizukami,T. *et al.* (2014) Molecular mechanisms underlying oncogenic RET fusion in lung adenocarcinoma. *J. Thorac. Oncol.*, **9**, 622–630.
20. Tsuta,K. *et al.* (2014) RET-rearranged non-small-cell lung carcinoma: a clinicopathological and molecular analysis. *Br. J. Cancer*, **110**, 1571–1578.
21. Pan,Y. *et al.* (2014) ALK, ROS1 and RET fusions in 1139 lung adenocarcinomas: a comprehensive study of common and fusion pattern-specific clinicopathologic, histologic and cytologic features. *Lung Cancer*, **84**, 121–126.
22. Gautschi,O. *et al.* (2013) A patient with lung adenocarcinoma and RET fusion treated with vandetanib. *J. Thorac. Oncol.*, **8**, e43–e44.

Received May 29, 2014; revised July 10, 2014; accepted July 19, 2014

A Three-microRNA Signature Predicts Responses to Platinum-Based Doublet Chemotherapy in Patients with Lung Adenocarcinoma

Motonobu Saito^{1,2}, Kouya Shiraishi¹, Kenji Matsumoto³, Aaron J. Schetter⁴, Hiroko Ogata-Kawata¹, Naoto Tsuchiya¹, Hideo Kunitoh⁵, Hiroshi Nokihara⁶, Shun-ichi Watanabe⁷, Koji Tsuta⁸, Kensuke Kumamoto², Seiichi Takenoshita², Jun Yokota^{1,9}, Curtis C. Harris⁴, and Takashi Kohno¹

Abstract

Purpose: To examine the clinical utility of intratumor microRNAs (miRNA) as a biomarker for predicting responses to platinum-based doublet chemotherapy in patients with recurring lung adenocarcinoma (LADC).

Experimental Design: The expression of miRNAs was examined in LADC tissues surgically resected from patients treated with platinum-based doublet chemotherapy at the time of LADC recurrence. Microarray-based screening of 904 miRNAs followed by quantitative reverse transcription-PCR-based verification in 40 test cohort samples, including 16 (40.0%) responders, was performed to identify miRNAs that are differentially expressed in chemotherapy responders and nonresponders. Differential expression was confirmed in a validation cohort ($n = 63$ samples), including 18 (28.6%) responders. An miRNA signature that predicted responses to platinum-based doublet chemotherapy was identified and its accuracy was examined by principal component and support vector machine analyses. Genotype data for the *TP53-Arg72Pro* polymorphism, which is associated with responses to platinum-based doublet chemotherapy, were subsequently incorporated into the prediction analysis.

Results: A signature comprising three miRNAs (miR1290, miR196b, and miR135a*) enabled the prediction of a chemotherapeutic response (rather than progression-free and overall survival) with high accuracy in both the test and validation cohorts (82.5% and 77.8%). Examination of the latter was performed using miRNAs extracted from archived formalin-fixed paraffin-embedded tissues. Combining this miRNA signature with the *TP53-Arg72Pro* polymorphism genotype marginally improved the predictive power.

Conclusion: The three-miRNA signature in surgically resected primary LADC tissues may be clinically useful for predicting responsiveness to platinum-based doublet chemotherapy in patients with LADC recurrence. *Clin Cancer Res*; 20(18); 4784–93. ©2014 AACR.

Introduction

Lung adenocarcinoma (LADC) is the most common type of non-small cell lung cancer (NSCLC) and is a leading cause of cancer mortality worldwide (1). Surgical resection is the best curative treatment for NSCLC; however, patients that experience recurrence after surgery and those with advanced disease receive chemotherapy to slow tumor growth and improve survival. LADCs harboring an *EGFR* mutation or an *ALK* fusion are primarily treated with specific tyrosine kinase inhibitors (TKI), with response rates of approximately 60% (2, 3). Other oncogene aberrations, such as *BRAF*, *HER2*, *RET*, and *ROS1*, are also targeted by specific TKIs (4–6), but a major barrier to curative treatment of LADC using TKIs is innate and acquired drug resistance (7, 8). Furthermore, more than 60% of USA/European and more than 30% of Japanese LADC cases do not harbor the oncogene aberrations listed above (9, 10). Such resistant and oncogene-negative LADC cases are treated with

¹Division of Genome Biology, National Cancer Center Research Institute, Tokyo, Japan. ²Department of Organ Regulatory Surgery, Fukushima Medical University School of Medicine, Fukushima, Japan. ³Department of Allergy and Immunology, National Research Institute for Child Health and Development, Setagaya, Tokyo, Japan. ⁴Laboratory of Human Carcinogenesis, Center for Cancer Research, National Cancer Institute, NIH, Bethesda, Maryland. ⁵Department of Medical Oncology, Japanese Red Cross Medical Center, National Cancer Center Hospital, Tokyo, Japan. ⁶Division of Thoracic Oncology, National Cancer Center Hospital, Tokyo, Japan. ⁷Division of Thoracic Surgery, National Cancer Center Hospital, Tokyo, Japan. ⁸Division of Pathology and Clinical Laboratories, National Cancer Center Hospital, Tokyo, Japan. ⁹Cancer Genome Biology, Institute of Predictive and Personalized Medicine of Cancer, Barcelona, Spain.

Note: Supplementary data for this article are available at Clinical Cancer Research Online (<http://clincancerres.aacrjournals.org/>).

Corresponding Author: Takashi Kohno, Division of Genome Biology, National Cancer Center Research Institute, 1-1 Tsukiji 5-chome, Chuo-ku, Tokyo, Japan 104-0045. Phone: 81-3-3542-2511; Fax: 81-3-3542-0807; E-mail: tkkohno@ncc.go.jp

doi: 10.1158/1078-0432.CCR-14-1096

©2014 American Association for Cancer Research.

Translational Relevance

The use of biomarkers to identify patients that will respond to platinum-based doublet chemotherapy before treatment is a critical strategy for improving the efficacy of chemotherapy for lung adenocarcinoma (LADC). Here, we report that the expression profile of three miRNAs in surgically resected primary tissues is clinically useful for predicting responsiveness to platinum-based doublet chemotherapy in patients with LADC recurring after initial surgical resection. This three-miRNA signature may be useful for the clinical management of LADC.

chemotherapy. The standard regimens comprise platinum-based doublets, that is, a combination of platinum and another agent; the drugs paired with platinum (cisplatin or carboplatin) include microtubule-targeted agents (paclitaxel, docetaxel, or vinorelbine) and DNA-damaging agents (gemcitabine or irinotecan). A series of trials in unselected patients revealed that the efficacy of each combination is similar, with response rates of 30% to 40% (11–13); thus, identifying biomarkers that can discriminate between patients that will respond to platinum-based doublet chemotherapy and those who may not before treatment will help improving the efficacy of chemotherapy for LADC.

microRNAs (miRNA) are small noncoding RNAs that posttranscriptionally regulate the translation of target genes; these miRNAs show altered expression in a variety of cancers and can modify the malignant properties of cancer cells, including the response to DNA damage (14–16). In fact, functional studies in LADC cell lines have identified a number of miRNAs that modulate sensitivity to platinum-based agents (17–23). Furthermore, miRNAs are stable in formalin-fixed paraffin-embedded (FFPE) tissues, that is, materials used for daily pathologic diagnosis (24, 25). Indeed, intratumor miRNA expression is a promising prognostic marker in patients that have undergone surgical resection (26–31), but few studies have examined the utility of miRNAs as a predictor of chemotherapeutic responses (32). To the best of our knowledge, only two such studies have been reported: one shows that a two-miRNA signature (miR149 and miR375) is associated with responses to platinum-based chemotherapy in NSCLC ($n = 38$), and the other shows that miR92a-2* expression is associated with chemoresistance in small-cell lung cancer ($n = 34$; refs. 33, 34).

Here, we investigated the utility of intratumor miRNAs as a biomarker for predicting responses to platinum-based doublet chemotherapy. We examined the expression of miRNAs in 103 surgically resected specimens obtained from patients who received platinum-based chemotherapy upon LADC recurrence to ascertain whether miRNA expression in primary tumors could predict responses to platinum-based doublet chemotherapy in patients who experienced LADC recurrence after surgery. First, a two-step screening process

involving 904 miRNAs was performed to identify an miRNA signature with predictive value. The first step was performed using a test cohort comprising 40 frozen tumor samples from which RNAs were isolated, and the second step was performed using a validation cohort comprising 63 cases, for which RNAs from FFPE tissues were available. We identified a three-miRNA signature that predicted responses to platinum-based doublet chemotherapy with an accuracy of >75%.

Materials and Methods**Materials**

Of note, 103 surgically resected LADC tissues were examined in the present study (Fig. 1A). Briefly, 643 Japanese patients with NSCLC received platinum-based doublet chemotherapy at the National Cancer Center Hospital (NCCH; Tokyo, Japan), between 2000 and 2008, and the therapeutic response was evaluated using the Response Evaluation Criteria In Solid Tumors (RECIST) guidelines (35). None of the patients had received prior treatment with platinum-based chemotherapy. Of the 643 cases, 118 were recurrent cases that had undergone surgical resection at NCCH, and all were pathologically diagnosed with adenocarcinoma. Tumor tissues for RNA extraction were available for 103 of 118 cases; these cases were examined in the present study. Information regarding age, gender, pathologic TNM stage (the 7th classification), smoking habits, postoperative chemotherapy regimens and responses to platinum doublet

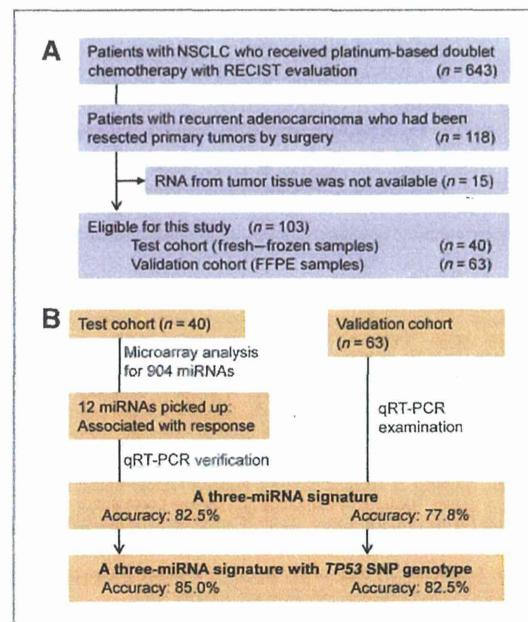


Figure 1. Patients and treatment strategy. A, selection of eligible cases, that is, 103 surgically resected cases that received platinum-based doublet chemotherapy upon LADC recurrence. B, identification and evaluation of a three-miRNA signature for the prediction of responses to chemotherapy.

therapy, and performance status (PS) were retrospectively collected. RNAs isolated from fresh-frozen tissues were available for 40 of 103 cases; these were defined as the test cohort. The RNAs from the test cohort were subjected to miRNA microarray analysis followed by verification by quantitative reverse transcriptase-PCR (qRT-PCR) analysis. RNAs from FFPE tissues were available for the remaining 63 cases; these were defined as the validation cohort. In addition, patients were classified into two categories according to RECIST guidelines: those that responded to platinum-based doublet chemotherapy [complete response (CR) or partial response (PR)] and those that did not [stable disease (SD) or progressive disease (PD)].

RNA extraction

RNA was extracted from snap-frozen tissues (test cohort) using TRizol reagent (Thermo Fisher Scientific). The quality and quantity of the RNAs were examined using a Bioanalyzer (Agilent). All RNA samples showed an RNA integrity number RIN >6.0; therefore, they were subjected to microarray analysis. For the validation cohort, RNA was isolated from three unstained FFPE sections (5- μ m thick). The area of the carcinoma in the three unstained sections was outlined by referring to a sequential section that was stained with hematoxylin and eosin. Each marked area was macrodissected using a sterile disposable scalpel and RNA was isolated using the Recover-All Total Nucleic Acid Isolation Kit (Ambion). Total RNA was quantified using a NanoDrop ND-1000 spectrometer (Thermo Fisher Scientific). The optical density (OD) 260/280 and OD 260/230 ratios were used for quality control.

Microarray experiments

The Human miRNA Microarray Kit release 14 (8 \times 15 K; Agilent Technologies), covering 904 miRNAs, was used to screen for miRNAs in the test cohort samples ($n = 40$). Data were normalized and analyzed using GeneSpring GX software (version 12.5; TOMY Digital Biology). The fold change in expression was defined as the ratio of expression in responders to that in nonresponders. Normalized and raw expression data were deposited in the Gene Expression Omnibus at the National Center for Biotechnology Information (GSE56264).

Examination of driver oncogene aberrations

All 40 test cohort samples were also screened for oncogene fusions (*EML4-* and *KIF5B-ALK*, *KIF5B-* and *CCDC6-RET*; and *CD74-*, *EZR-*, and *SLC34A2-ROS1*) by reverse transcription-PCR as previously described (4, 36). Genomic DNA was extracted from fresh or frozen samples from all 103 subjects using a QIAamp DNA Mini Kit (QIAGEN) and then analyzed for *EGFR*, *KRAS*, *BRAF*, and *HER2* hot spot mutations using the high resolution melting method (37, 38).

qRT-PCR analysis

qRT-PCR of mature miRNA was performed using TaqMan MicroRNA assays (Thermo Fisher Scientific) and the 7900 HT Fast Real-Time PCR System (Thermo Fisher Scientific).

cdNA was synthesized using miRNA-specific primers and a TaqMan MicroRNA Reverse Transcription Kit (Thermo Fisher Scientific). RNA (40 ng) was reverse transcribed in a 20 μ L reaction containing gene-specific RT probes. All assays were performed in triplicate and investigators were blinded to the clinical outcome. All TaqMan probes were purchased from Thermo Fisher Scientific: hsa-miR135a-3p (ID 002232), hsa-miR196b-5p (ID 002215), hsa-miR1181 (Assay ID 241045_mat), hsa-miR31-5p (ID 002279), hsa-miR31-3p (ID 002113), hsa-miR1290 (ID 002863), hsa-miR598 (ID 001988), hsa-miR1 (ID 002222), hsa-miR144-5p (ID 002148), hsa-miR628-5p (ID 002433), hsa-miR449a (ID 001030), and hsa-miR34b-3p (ID 002102). RNU66 (ID 001002) was used as a normalization control. Relative expression of miRNAs was calculated using RQ manager 1.2 (Thermo Fisher Scientific).

Statistical analysis

Differences in miRNA expression levels between responders and nonresponders were tested by the Mann-Whitney *U* test using Graphpad Prism v5.0 (Graphpad Software Inc). Spearman correlation analysis was used to examine the correlation between microarray and qRT-PCR data (Graphpad Prism v5.0). Linear discriminant analysis was performed for each cohort to distinguish responders from nonresponders (JMP 10 software; SAS Institute) based on miRNA expression (i.e., the miRNA signature). Continuous expression values for a single miRNA or for plural miRNAs, that is, ΔC_t values obtained by qRT-PCR against RNU66, were included as variables in the analysis. Receiver operating characteristic (ROC) curves were generated to evaluate response sensitivity and the area under the curve (AUC) was calculated (JMP 10). Principal component analysis (PCA) of the expression of three miRNAs (miR1290, miR196b, and miR135a*) was performed using JMP 10.

Results

Sample selection

The aim of this study was to identify biomarkers in patients with metastatic LADC who relapsed following potential curative surgical resection. Therefore, surgically resected primary tumor tissues from 103 LADC patients who were treated with platinum-based doublet chemotherapy upon recurrence were selected for miRNA profiling (Fig. 1A). The cases were assigned to a test cohort ($n = 40$; RNAs from frozen tissue available) or a validation cohort ($n = 63$; RNAs from FFPE tissues available) according to the availability of tumor tissue samples. Patients in both cohorts were classified as responders (CR and PR) or nonresponders (SD and PD) to platinum-based doublet chemotherapy according to the RECIST criteria (Materials and Methods; Supplementary Table S1). In this study, platinum-based doublet chemotherapy includes several different regimens. The cohorts were similar in terms of clinicopathologic characteristics such as age, gender, smoking habits, pathologic stage, representative oncogene mutations, therapeutic regimen, and therapeutic response (Table 1). The samples